



**Title: Dopaminergic retinal cell loss and visual dysfunction in Parkinson's disease**

**Running head: Retinal dopaminergic cell loss in PD**

Isabel Ortuño-Lizarán PhD<sup>1</sup>, Xavier Sánchez-Sáez MSc<sup>1</sup>, Pedro Lax PhD<sup>1</sup>, Geidy E. Serrano PhD<sup>2</sup>, Thomas G. Beach MD, PhD<sup>2</sup>, Charles H. Adler MD, PhD<sup>3</sup>, Nicolás Cuenca PhD<sup>1,4</sup>

<sup>1</sup>Department of Physiology, Genetics and Microbiology, University of Alicante, Alicante, Spain

<sup>2</sup>Banner Sun Health Research Institute, Sun City, AZ, USA

<sup>3</sup>Mayo Clinic Arizona, Scottsdale, AZ, USA

<sup>4</sup>Institute Ramón Margalef, University of Alicante, Alicante, Spain

Corresponding author: Nicolás Cuenca, cuenca@ua.es

This article has been accepted for publication and undergone full peer review but has not been through the copyediting, typesetting, pagination and proofreading process which may lead to differences between this version and the Version of Record. Please cite this article as doi: 10.1002/ana.25897

## Abstract

**Objective:** Considering the demonstrated implication of the retina in PD pathology and the importance of dopaminergic cells in this tissue, we aimed to analyze the state of the dopaminergic amacrine cells and some of their main post-synaptic neurons in the retina of PD.

**Methods:** Using immunohistochemistry and confocal microscopy, we evaluated morphology, number, and synaptic connections of dopaminergic cells and their post-synaptic cells, AII amacrine and melanopsin-containing retinal ganglion cells, in control and PD eyes from human donors.

**Results:** In PD, dopaminergic amacrine cell number was reduced between 58% and 26% in different retinal regions, involving a decline in the number of synaptic contacts with AII amacrine cells (by 60%) and melanopsin cells (by 35%). Despite losing their main synaptic input, AII cells were not reduced in number, but they showed cellular alterations compromising their adequate function: i) a loss of mitochondria inside their lobular appendages, that may indicate an energetic failure and ii) a loss of connexin 36, suggesting alterations in the AII coupling and in visual signal transmission from the rod pathway.

**Interpretation:** The dopaminergic system impairment and the affection of the rod pathway through the AII cells may explain and be partially responsible for the reduced contrast sensitivity or electroretinographic response described in PD. Also, dopamine reduction and the loss of synaptic contacts with melanopsin cells may contribute to the melanopsin retinal ganglion cell loss previously described and to the disturbances in circadian rhythm and sleep reported in PD patients. These data support the idea that the retina reproduces brain neurodegeneration and is highly involved in PD pathology.

## Keywords

Parkinson's disease, human retina, dopaminergic cells, AII amacrine cells, contrast sensitivity, melanopsin

## Abbreviations

Inner Plexiform Layer: IPL

Melanopsin retinal ganglion cells: mRGC

Optical Coherence Tomography: OCT

Outer Nuclear Layer: ONL

Outer Plexiform Layer: OPL

## Introduction

Parkinson's disease (PD) is a common neurodegenerative disorder traditionally characterized by the presence of Lewy bodies in the brain and by the degeneration of mesencephalic dopaminergic neurons in the *substantia nigra pars compacta*, that leads to a depletion of dopamine in the *striatum* and to the subsequent motor alterations<sup>1</sup>. Although classically considered as a brain-predominant disease, recent growing evidence supports the involvement of peripheral and extracranial organs in PD. Among them, the retina has been recently proposed to reflect the PD brain pathology: phosphorylated- $\alpha$ -synuclein deposits, similar to Lewy bodies, have been found in the retina of PD patients, whose density correlated with disease severity<sup>2,3</sup>. In addition, PD patients present several visual symptoms such as reduced amplitudes in b-waves and oscillatory potentials in electroretinograms, reduced visual evoked potentials, inner retinal layer thinning by

optical coherence tomography (OCT)<sup>4</sup>, impaired motion perception, contrast sensitivity and color discrimination<sup>5-8</sup>, circadian rhythm dysfunction<sup>9,10</sup> and melanopsin-containing retinal ganglion cell (mRGC) degeneration<sup>11</sup>.

Considering the described similarities between the neurodegenerative process in the retina and brain, it is natural to wonder if the dopaminergic cells in the retina are involved in the disease as they are in the brain. In the retina, dopamine is an essential neuromodulator that has widespread influences on retinal function and regulation. Among their main functions, dopaminergic amacrine cells regulate the light/dark adaptation, modulating and reshaping retinal circuitries depending on light conditions. The sustained dopaminergic light responses are regulated by mRGC<sup>12,13</sup> and, at the same time, some mRGC are directly post-synaptic to dopaminergic amacrine cells<sup>14,15</sup>, creating a complex regulatory network.

Also, dopaminergic cells are involved in the regulation of the rod pathway through the coupling/uncoupling of the AII amacrine cells<sup>16</sup>. In scotopic conditions, AII amacrine cells are coupled with other AII cells and with ON cone bipolar cells by homotypic and heterotypic connexin 36 gap junctions<sup>17</sup>, and they add the rod-pathway information into the cone-pathway<sup>18</sup>. In photopic conditions, dopamine release is stimulated, and dopaminergic processes make synaptic contacts onto AII cell bodies and lobular appendages, uncoupling AII from their contacts<sup>19,20</sup>. Given its importance in regulating retinal function<sup>21</sup>, an impairment in the retinal dopaminergic system of PD patients may lead to severe retinal dysfunctions like those previously mentioned.

It is accepted that the retina is highly affected in PD but, whether or not dopaminergic amacrine cells degenerate in the retina of PD patients, as happens in the brain, remains unknown. The aim of this work is to analyze the state of the dopaminergic amacrine cells in the retinas of PD patients

compared to controls, and the relationship with their main post-synaptic neurons: AII amacrine cells and mRGC.

## **Materials and methods**

### **Source of human subjects and clinical characterization**

Retinas from human donors were obtained post-mortem from volunteers in the Arizona Study of Aging and Neurodegenerative Disorders (AZSAND)/ Banner Sun Health Research Institute Brain and Body Donation Program (BBDP; <https://www.brainandbodydonationprogram.org>)<sup>22</sup> and from the Hospital General Universitario de Alicante (HGUA). All procedures involving humans followed the Declaration of Helsinki (Code of Ethics of the World Medical Association) and were approved by the Ethics Committee of the University of Alicante (UA-2018-04-17). All participants signed written informed consent prior to their enrolment in AZSAND. Donors did not significantly differ in age, being from 69 to 88 years old at the time of death, and did not report previous ophthalmological pathologies. Participants in the study were clinically characterized by standard tests assessing neurological components as previously described<sup>23,24</sup>. Individuals diagnosed with Parkinson's disease belong to the PD group (n=8; 76.3±5.55 years old; AZSAND) and healthy individuals, without neurodegenerative or ocular diseases, to the control group (n=5; 72.6±1.9 years old; HGUA). ¿INCLUIR TABLA CON INFORMACION DE PACIENTES?

### **Retinal immunohistochemistry**

After enucleation, eyes were fixed in paraformaldehyde (3.75-4%) 2 h at RT or 24-72 h at 4 °C. Then, they were washed in 0.1 M phosphate buffer and cryoprotected in 15%, 20% and 30% successive sucrose solutions. Cornea, iris, lens and vitreous body were extracted, and the retina

was dissected into eight pieces. The superonasal and the temporal-central pieces were employed for subsequent wholemount analysis. In other cases, the temporal-central region was cut in a cryostat to obtain vertical sections of 14 microns. Immunohistochemistry in wholemount retinas and vertical sections was performed following previously described protocols<sup>2</sup>. Briefly, retinas were washed three times in 0.1 M phosphate buffer and incubated with the primary antibody overnight or for 3 nights (in cuts and wholemounts, respectively). Primary antibodies used were sheep polyclonal to tyrosine hydroxylase (1:200; AB1542 Merck Millipore, Darmstadt, Germany), rabbit polyclonal anti-calretinin (1:200; CR7679 Swant, Marly, Switzerland), mouse polyclonal anti-cytochrome C (1:100; Zymed, San Francisco, CA, USA), mouse polyclonal anti-connexin 36 (1:200; MAB3045 Merck Millipore, Darmstadt, Germany) and rabbit polyclonal anti-melanopsin (1:1000; UF028 kindly provided by Dr. Ignacio Provencio, University of Virginia, Charlottesville, VA, USA)<sup>25</sup>. After the incubation time, they were washed and incubated with secondary antibodies at a dilution 1:100 for 1 h or 2 nights in cuts or in wholemounts, respectively. The polyclonal secondary antibodies used were: donkey anti-rabbit conjugated to Alexa-555 (A31572), donkey anti-sheep conjugated to Alexa-488 (A11015), and donkey anti-mouse conjugated to Alexa-488 (A21201; all from ThermoFisher Scientific, Rockford, USA). Samples were washed again, wholemount retinas were disposed with the ganglion cell layer side up, and all samples were mounted in Citifluor (Citifluor Ltd, London, UK) and coverslipped. Fluorescence images were obtained using a Leica confocal microscope TCS SP8 (Leica Microsystems, Wetzlar, Germany).

### **Antibody characterization**

The sheep polyclonal anti-tyrosine hydroxylase (AB1542, Merck Millipore) was generated against the native tyrosine hydroxylase protein from rat pheochromocytoma and it has been previously characterized by immunohistochemistry in the rat and mouse retina<sup>26,27</sup>. Its staining

Accepted Article

pattern in the human retina is comparable to that of other species such as squirrel, cat, or rat<sup>20,26,28</sup>, and the density and distribution of control human dopaminergic cells when stained with this antibody is comparable to previous studies done in other primates<sup>29,30</sup>. Also, the dopaminergic staining pattern observed is the same as the obtained with other anti-tyrosine hydroxylase antibodies (ab112, Abcam, Cambridge, UK, data not shown).

The rabbit polyclonal anti-calretinin (CR7679, Swant) was produced by immunization with recombinant human calretinin containing a 6-his tag at the N-terminal. The manufacturer provides its characterization by western blot on brain lysates and by immunohistochemistry in mice brain, and it has also been characterized by immunohistochemistry in the human retina<sup>31</sup>.

The mouse polyclonal anti-cytochrome C (Zymed) was generated against the rat cytochrome C protein and has been previously characterized by immunohistochemistry in the human retina<sup>32</sup>.

The mouse polyclonal anti-connexin 36 (MAB3045, Merck Millipore) was produced against the perch connexin 35 and, according to the manufacturer, recognizes primate connexin 36, the gene homologue to connexin 35. It has been previously characterized by immunohistochemistry in the retina<sup>33</sup>.

Finally, the rabbit polyclonal anti-melanopsin antiserum (gift from Dr. Provencio) was raised against the 15 N-terminal amino acids of the human melanopsin protein and has been characterized by immunohistochemistry in the human retina<sup>11,34</sup>.

### **Cellular quantification**

Confocal images of flat retinas were used to assess the morphology and density of dopaminergic and AII amacrine cells, and the number of connections between dopaminergic and AII amacrine cells or mRGC. Photographs of wholemount retinas were obtained using the tiles module in a TCS SP8 Leica confocal. The total number of dopaminergic or AII amacrine cells was counted

in the whole retinal quadrant, the area of the quadrant was measured, and the density of cells per  $\text{mm}^2$  was calculated as the number of cells/area of retina. The area of the measured retinal pieces ranged from 80 to 150  $\text{mm}^2$  in the central-temporal quadrant and from 32 to 97  $\text{mm}^2$  in the superonasal quadrants. Density maps of dopaminergic cells in the temporal-central quadrant and in a representative area of the superonasal quadrant were made using the ggplot2<sup>35</sup> package in R version 3.6 (R Core Team 2019).

The number of dopaminergic contacts with AII cells was measured in, at least, 20 frames randomly distributed in each retina and expressed as the number of contacts per AII cell. The number of dopaminergic contacts with melanopsin dendrites was counted and divided per dendrite length, calculating the value of dopaminergic contacts per 100  $\mu\text{m}$  of melanopsin dendrites in, at least, 15 frames randomly distributed per retina.

### **Statistical analysis**

Statistical analysis was performed using the GraphPad Prism software (version 6; Graph-Pad Software Inc., San Diego, CA). Non-parametric two-tailed Mann-Whitney tests were used to determine the differences of the analyzed variables between the two groups considered: PD and control. Values are presented in boxplots made using the ggplot2<sup>35</sup> package: the box shows the interquartile range and the line dividing the box represents the median of the data. In all cases, the significance level was set at  $P < 0.05$ .

## **Results**

### **Dopaminergic cell degeneration**

Dopamine-containing cells in the retina of healthy subjects are wide field amacrine cells that extend their thin and ramified dendrites long distances creating a dense plexus<sup>36</sup>. Dopaminergic



cells frequently make contacts with the soma of their post-synaptic neurons at the S1 strata of the inner plexiform layer (IPL). In healthy individuals, this high density of contacts around post-synaptic cell bodies creates ring-like structures that can be observed in the dopaminergic plexus (Fig. 1A, arrows). Due to their wide retinal neuromodulatory function, dopaminergic dendrites not only stratify at the S1 strata (Fig. 1C), but also, although to a lesser extent, at the IPL S3, and even S5 (Fig. 1C, arrowheads), and at the outer plexiform layer (OPL) and outer nuclear layer (ONL) (Fig. 1C, arrows) reaching photoreceptor cell bodies.

By contrast, in PD (Fig. 1B, D), dopaminergic cells display some characteristics of an atrophied morphology: dendrites are shorter and thicker, with some swollen fragments (Fig. 1B, arrowheads) and their plexus has lost the typical ring structure. Also, almost all the remaining dendrites are located at the S1 (Fig. 1D) and very few of them reach the OPL, ONL (Fig. 1D, arrows) the S3 or the S5 (Fig. 1D, arrowheads), probably inducing a loss of dopamine in these regions.

In healthy primates, dopaminergic amacrine cell distribution is equivalent in all quadrants, as they are symmetrically distributed around the fovea. They are bigger and sparsely distributed in the periphery and of smaller size and higher density towards the central retina, reaching their maximum density peak at the parafovea<sup>29,30</sup>. Fig. 2 shows color-coded density maps where the white or black dots are the dopaminergic cells, yellow shows the maximum density, and dark blue shows the minimum dopaminergic cell density. In controls, dopaminergic cell distribution is comparable to the previously described: there is a maximum density peak at the parafovea, with 45 cells/mm<sup>2</sup>, that rapidly declines concentrically towards more peripheral locations: in the perifovea, the median density is 30 cells/mm<sup>2</sup> and in the near periphery (next 3mm from perifovea; 0-3mm to perifovea in Fig. 2) is 18 cells/mm<sup>2</sup> (Fig. 2A, E). The effect of eccentricity in dopaminergic density is also observed in the superonasal quadrant (Fig. 2F, H), where the median

dopaminergic cell density is 19 cells/mm<sup>2</sup> in the most central region and declines to 17 cells/mm<sup>2</sup> and 14 cells/mm<sup>2</sup> towards the periphery.

In addition to an altered morphology, PD retinas also display a decrease in the dopaminergic cell density. Notice that dopaminergic cell density is higher in controls than in PD in the whole central quadrant (20.2 cells/mm<sup>2</sup> in controls vs 13.1 cells/mm<sup>2</sup> in PD) (Fig. 2A-B, E), with strong differences in the parafoveal and perifoveal regions. In the parafovea (insets in Fig. 2A-B), dopaminergic cell density in PD is reduced by a 58% (45.1 cells/mm<sup>2</sup> in controls vs 19.2 cells/mm<sup>2</sup> in PD) and in the perifovea by a 51% (29.7 cells/mm<sup>2</sup> in controls vs 14.4 cells/mm<sup>2</sup> in PD) (Fig. 2E). Fig. 2C-D shows confocal images of control and PD dopaminergic cells at the parafovea, where the cell number reduction can be easily observed. No statistical analysis has been done in this quadrant due to the small sample size, caused by the difficulty of obtaining human fovea tissue.

In the superonasal quadrant, the dopaminergic cell density was reduced by 45%, changing from 18.4 cells/mm<sup>2</sup> in controls to 10.8 cells/mm<sup>2</sup> in PD retinas ( $P<0.01$ ) (Fig. 2F-H). This decrease was statistically significant thorough the whole quadrant, from the most central to the most peripheral regions. In the most central area (from 2 to 7mm to the optic nerve) the median dopaminergic cell density changed from 19.4 cells/mm<sup>2</sup> in healthy subjects to 13.4 cells/mm<sup>2</sup> in PD patients ( $P<0.05$ ). Towards the periphery, dopaminergic cell density decreases in both groups and the differences are maintained: 17.3 cells/mm<sup>2</sup> in controls are reduced to 12.8 cells/mm<sup>2</sup> in PD in the region between 7 to 11mm to the optic nerve ( $P<0.05$ ), and, in the most peripheral area (from 11 to 16 mm to the optic nerve), 14.4 cells/mm<sup>2</sup> in controls change to 8.8 cells/mm<sup>2</sup> in PD ( $P<0.01$ ) (Fig. 2F-H).

### **Morphological alterations of AII amacrine cells**

Double immunostaining using tyrosine hydroxylase (green) and calretinin (red) antibodies allowed visualizing the relationship between dopaminergic amacrine cells and their main post-synaptic neurons: AII amacrine cells. Synaptic contacts from dopaminergic cells to AII amacrine cells are so abundant that they make ring-like structures around the cell body (Fig. 3A). In PD, probably as a result of the dopaminergic cell degeneration, ring-like structures around AII amacrine cells are partially lost (Fig. 3B). The quantification of dopaminergic synaptic contacts per AII cell body revealed that these synaptic connections are reduced by 60% (from 9.3 to 3.7) in PD patients (Fig. 3C-G). But, despite losing one of their major inputs, AII amacrine cell number remains stable in PD compared to controls (Fig. 3H).

The maintenance of AII amacrine cell number does not discard the possibility that they are morphologically or functionally affected by the disease. In order to address this issue, characteristic structural features of AII cells, as well as functional implications were assessed.

In healthy individuals, AII cells are small amacrine cells whose dendrites stratify close to the cell body in both *sublamina* a (OFF) and b (ON) of the IPL (Fig. 4A) while in PD their typical morphology and stratification has been partially loss (Fig. 4B). Also, in normal conditions, AII cells contain big mitochondria within their lobular appendages that supply them with the energy required for their adequate function. Mitochondria (green) inside the AII lobular appendages (red) can be observed as yellow dots (arrows) in Fig. 3. These mitochondria are big and abundant in control subjects (Fig. 4A, C, E) but they may be affected in PD (Fig. 4B, D, F): the yellow dots are less abundant and, when present, they are much smaller than in control retinas.

Another important characteristic of AII amacrine cells is that, in dark conditions, they are coupled to each other and to ON cone bipolar cells by gap junctions. These gap junctions are mediated by connexin 36 protein and are located at the ON *sublamina* of IPL. Fig. 4 shows co-immunostaining of AII cells (red) and connexin 36 (green) in retinas of control and PD subjects. In controls (Fig.

5A, C, E, G), connexin 36 at AII amacrine cells is abundant and mainly located in the S4 and S5 strata of the IPL (ON *sublamina*). Nevertheless, in PD (Fig. 5B, D, F, H), the amount of connexin 36 immunostaining in the ON *sublamina* is strongly reduced.

### **Reduced dopaminergic synaptic contacts in melanopsin-containing retinal ganglion cells**

Some mRGC types are post-synaptic to dopaminergic amacrine cells, especially the ones that stratify in the IPL OFF *sublamina* (M1 and displaced M1). Double immunohistochemistry using antibodies against tyrosine hydroxylase (green) and melanopsin (red) revealed the synaptic relationship between dopaminergic and mRGC in the IPL (Fig. 6). The above-mentioned loss of the dopaminergic plexus and the previously described impairment of mRGC<sup>11</sup> in PD can be observed in Fig. 6, where the dopaminergic plexus (in green) is reduced and the mRGC morphology (in red) is altered in PD (lower dendritic complexity, shorter dendrites, and reduced number of ramifications) (Fig. 6B, D) compared to controls (Fig. 6A, C). In healthy subjects, dopaminergic cells make abundant synapses with mRGC dendrites, observed as green dots contacting the melanopsin dendrites (in red) in Fig. 6E, F (arrowheads). Nevertheless, probably as a consequence of the reduced dopaminergic plexus, the dopaminergic contacts that reach mRGC are reduced in PD, although still present (Fig. 6G, H, arrowheads). The numerical quantification of these contacts reveals a 35% decrease in PD, changing from 70 contacts per 100  $\mu\text{m}$  in controls to 43 contacts per 100  $\mu\text{m}$  in PD ( $P < 0.0001$ ) (Fig. 6I).

### **Discussion**

This study provides, for the first time, a systematic quantification of retinal dopaminergic cells in PD patients, demonstrating a loss of these cells and their plexus, involving a global impairment of the dopaminergic system. As dopamine is both a neurotransmitter and a broad neuromodulator

in the retina<sup>37,38</sup>, its loss may cause cellular and functional alterations at very different levels. At the S1 strata, dopaminergic cells make direct synaptic contacts with AII, A8, A17 and A13 amacrine cells<sup>20,39,40</sup>, at the OPL, they regulate the horizontal cell coupling and the cone-rod coupling<sup>37,38</sup>, and they also modulate ganglion cells through direct (as is the case for mRGC) or diffuse dopaminergic regulation<sup>40,41</sup>. Among all of their post-synaptic cells, special attention has been given to the AII amacrine cells, involved in the rod pathway<sup>41-44</sup>.

Dopaminergic cells and their synaptic contacts to AII amacrine cells are strongly reduced in PD. But, although lacking one of their main inputs, AII cell number remains stable. The fact that AII cells survive while dopaminergic cells are lost may be interpreted in different ways. First, it may reflect that degeneration in PD is somehow specific and preferentially affects specific cell types, like dopaminergic or mRGC<sup>11</sup>. Second, it is possible that the remaining dopamine levels, together with additional AII inputs coming from cone and rod bipolar and other amacrine cells<sup>44-46</sup>, are enough to maintain the AII cell number. Third, AII cells may be more resistant to this type of neurodegeneration but may eventually degenerate if the disease is prolonged in time or of higher severity. Finally, a combination of these three hypotheses may be occurring, and time-course studies of PD progression would be needed to clarify this.

Although AII cells remain, some of their essential cellular components are impaired in the disease, which may be reflected in functional alterations. The big mitochondria in their lobular appendages are lost or reduced in size, indicating an energetic failure of AII cells in PD. Also, the amount of connexin 36 in the IPL ON *sublamina* is decreased, revealing a failure in AII coupling through gap junctions and suggesting a functional impairment in the transmission of the rod-mediated visual signals<sup>17</sup>: if AII cells have a reduced ability to couple, the integration of the rod pathway information into the cone pathway would be deficient. In normal conditions, the reduction of dopamine levels during dark hours results in increasing AII coupling<sup>16,40,41</sup>. In PD, two possible

processes may have occurred: 1) as a result of dopamine loss, AII cells are continuously coupled, which induces down-regulation of connexin 36 expression and/or energetic unbalance accompanied by mitochondrial failure, 2) as PD reduces mitochondrial viability<sup>47</sup>, AII mitochondria may be lost as a direct consequence of the disease and induce a functional impairment of AII cells losing their coupling proteins. Again, time-course research is needed to understand the progression and relationship of the cellular changes observed.

Dopaminergic cells also play an important role in regulating the retinal dark to light adaptation and the circadian rhythm<sup>40</sup>. In a bidirectional way, the sustained dopaminergic response to light is regulated by mRGC<sup>12,13</sup> and, at the same time, mRGC in the IPL *sublamina* OFF are directly post-synaptic to dopaminergic cells and are subjected to dopaminergic modulation<sup>14,15</sup>. Thus, considering the close relationship between dopamine and mRGC, the dopaminergic cell degeneration and the loss of synaptic contacts reported here may be one of the causes of the impairment of mRGC described in the disease and may contribute to the circadian rhythm dysfunction and sleep problems reported in patients<sup>11</sup>. In a retrograde way, the loss of the mRGC may also accelerate the dopaminergic degeneration.

Our results are in accordance with previous data that suggested a possible role of dopaminergic retinal cells in PD<sup>48-50</sup>. The levels of retinal dopamine are decreased in patients<sup>50</sup> and in MPTP-treated rabbits<sup>51</sup> and monkeys<sup>52</sup>. Also, the degeneration of dopaminergic amacrine cells has been described in PD animal models, such as MPTP-treated mice<sup>53-55</sup> and monkeys<sup>56</sup>, rotenone-treated rats<sup>57,58</sup>, 6-OHDA-treated rats<sup>59</sup> and mice overexpressing  $\alpha$ -synuclein<sup>60</sup>. This first systematic study regarding dopaminergic amacrine cells in the human retina of PD patients demonstrates that animal models previously used in the literature accurately reflect the state of the dopaminergic system in the retina, since they present similar alterations, and indicate that these models are useful for further studies.

Nevertheless, in contrast with what happens in the brain, previous studies had not found phosphorylated- $\alpha$ -synuclein deposits within retinal dopaminergic cells in patients suffering from PD<sup>2,3,61</sup>. We and others have always found scarce and sparse retinal phosphorylated- $\alpha$ -synuclein deposits in the ganglion cell layer, and never within dopaminergic cells. This fact suggests that dopaminergic cell death in the retina is independent of a self-accumulation of phosphorylated- $\alpha$ -synuclein or that the levels of phosphorylated- $\alpha$ -synuclein are low and the techniques used are not able to detect it.

Overall, the present results suggest that the retina is highly affected during PD neurodegeneration. This retinal impairment may explain some of the visual deficits described in patients. For example, altered coupling and uncoupling of the horizontal cells as a result of the dopaminergic impairment may underlie the diminished contrast sensitivity described in patients<sup>6,62-64</sup> and the ERG oscillatory potentials reduction may reflect alterations in dopaminergic cells and/or in their interactions with other amacrine, bipolar and ganglion cells<sup>7</sup>. In addition, as Müller and bipolar cells also present dopamine receptors<sup>65</sup>, they are subjected to dopamine modulation: lower dopamine levels may be involved in the reduction of the ERG b-wave (that mainly reflects the state of bipolar cells and their interaction with Müller cells) observed in patients<sup>7</sup> or after dopamine receptor blockage<sup>66</sup>. Also, the loss of connexin 36 described in the present work and the consequent impairment in signal transmission from the rod to the cone pathway<sup>17</sup> may cause alterations in cone bipolar cells activity, probably affecting the ERG b-wave. Finally, using OCT, some authors have described a thinning of the nerve fiber layer<sup>67</sup>, nerve fiber layer + ganglion cell layer + IPL<sup>49</sup>, or ganglion cell layer + IPL<sup>4</sup>, and this suggests a possible role of dopamine deficiency in the structural remodeling of these bands, although the current data is still inconclusive and other authors have not found these changes<sup>7</sup>.

Accepted Article

Interestingly, it has recently been proposed that retinal affection may have important implications not only in visual dysfunctions but also in some of the motor symptoms. Willis and colleagues<sup>68</sup> have observed that animal models intravitreally injected with minimal doses of MPTP, 6OHDA, rotenone or paraquat, displayed motor impairment without having brain affection. Other studies using L-DOPA in the retina showed an improvement of the motor symptoms<sup>69</sup>, and so did timed light therapy that, besides enhancing sleep, mood and anxiety, also improved motor function<sup>70</sup> probably by a dopamine release stimulation and by partially restoring circadian rhythms through mRGC function improvement<sup>71,72</sup>.

In conclusion, the dopaminergic system, which involves the dopaminergic amacrine cells and their post-synaptic cells, is affected in PD and this retinal degeneration may explain not only visual but also motor and circadian rhythm alterations suffered by PD patients. Thus, eye care and protection to preserve retinal cells, retinal pharmacological treatment, or chronotherapies to stimulate mRGC and retinal dopamine release, may have a positive impact in the disease progression. Also, visual exams should be considered during PD diagnosis and follow-up, as visual changes may partially reflect the retinal state and hence the PD neurodegenerative process. This study also reinforces the idea that retinal pathology may be considered as a biomarker of Parkinson disease.

### **Acknowledgements**

This work was supported by the Michael J. Fox Foundation for Parkinson's Research. IOL and XSS acknowledge financial support from the Ministerio de Educación, Spain (FPU 14/03166; FPU 16/04114). NC acknowledges financial support from the Ministerio de Economía y Competitividad, Spain (MINECO-FEDER-BFU2015-67139-R), Instituto de Salud Carlos III



(RETICS-FEDER RD16/0008/0016), Asociación Retina Asturias, and Generalitat Valenciana-FEDER (IDIFEDER/2017/064). The Brain and Body Donation Program has been supported by the National Institute of Neurological Disorders and Stroke (U24 NS072026), the National Institute on Aging (P30 AG19610), the Arizona Department of Health Services, the Arizona Biomedical Research Commission, and the Michael J. Fox Foundation for Parkinson's Research.

**Author Contributions:** IOL, TB, CA and NC contributed to the conception and design of the study; IOL, XSS, PL, GS, contributed to the acquisition and analysis of data; IOL, XSS, PL, GS, TB, CA and NC contributed to drafting the text and preparing the figures.

**Potential Conflicts of Interest:** The authors declare that they have no conflict of interest.

## References

1. Lotharius J, Brundin P. Pathogenesis of Parkinson's disease: dopamine, vesicles and alpha-synuclein. *Nat. Rev. Neurosci.* 2002;3(12):932–942.
2. Ortuño-Lizarán I, Beach TG, Serrano GE, et al. Phosphorylated  $\alpha$ -Synuclein in the Retina is a Biomarker of Parkinson's Disease Pathology Severity. *Mov. Disord.* 2018;33(8):1315–1324.
3. Veys L, Vandenabeele M, Ortuño-Lizarán I, et al. Retinal  $\alpha$ -synuclein deposits in Parkinson's disease patients and animal models. *Acta Neuropathol.* 2019;137(3):379–395.
4. Chrysou A, Jansonius NM, van Laar T. Retinal layers in Parkinson's disease: A meta-analysis of spectral-domain optical coherence tomography studies. *Parkinsonism Relat. Disord.* 2019;64:40–49.

5. Langheinrich T, Tebartz Van Elst L, Lagrèze WA, et al. Visual contrast response functions in Parkinson's disease: Evidence from electroretinograms, visually evoked potentials and psychophysics. *Clin. Neurophysiol.* 2000;111(1):66–74.
6. Lin TP, Rigby H, Adler JS, et al. Abnormal visual contrast acuity in Parkinson's disease. *J. Parkinsons. Dis.* 2015;5(1):125–30.
7. Nowacka B, Lubiński W, Honczarenko K, et al. Bioelectrical function and structural assessment of the retina in patients with early stages of Parkinson's disease (PD). *Doc. Ophthalmol.* 2015;131(2):95–104.
8. Bohnen NI, Haugen J, Ridder A, et al. Color discrimination errors associate with axial motor impairments in Parkinson's Disease. *Mov. Disord. Clin. Pract.* 2017;4(6):864–869.
9. Gros P, Videnovic A. Overview of Sleep and Circadian Rhythm Disorders in Parkinson Disease. *Clin. Geriatr. Med.* 2020;36(1):119–130.
10. Leng Y, Musiek ES, Hu K, et al. Association between circadian rhythms and neurodegenerative diseases. *Lancet. Neurol.* 2019;18(3):307–318.
11. Ortuño-Lizarán I, Esquiva G, Beach TG, et al. Degeneration of human photosensitive retinal ganglion cells may explain sleep and circadian rhythms disorders in Parkinson's disease. *Acta Neuropathol. Commun.* 2018;6(1):1–10.
12. Zhang D-Q, Wong KY, Sollars PJ, et al. Intraretinal signaling by ganglion cell photoreceptors to dopaminergic amacrine neurons. *Proc. Natl. Acad. Sci. U. S. A.* 2008;105(37):14181–14186.
13. Prigge CL, Yeh P-T, Liou N-F, et al. M1 ipRGCs Influence Visual Function through Retrograde Signaling in the Retina. *J. Neurosci.* 2016;36(27):7184–7197.
14. Van Hook MJ, Wong KY, Berson DM. Dopaminergic modulation of ganglion-cell

photoreceptors in rat. *Eur. J. Neurosci.* 2012;35(4):507–518.

15. Liao HW, Ren X, Peterson BB, et al. Melanopsin-expressing ganglion cells on macaque and human retinas form two morphologically distinct populations. *J. Comp. Neurol.* 2016;524(14):2845–2872.
16. Hampson EC, Vaney DI, Weiler R. Dopaminergic modulation of gap junction permeability between amacrine cells in mammalian retina. *J. Neurosci.* 1992;12(12):4911–4922.
17. Deans MR, Volgyi B, Goodenough DA, et al. Connexin36 is essential for transmission of rod-mediated visual signals in the mammalian retina. *Neuron* 2002;36(4):703–712.
18. Nelson R, Kolb H. Amacrine cells in scotopic vision. *Ophthalmic Res.* 1984;16(1–2):21–26.
19. Mariani AP, Kolb H, Nelson R. Dopamine-containing amacrine cells of rhesus monkey retina parallel rods in spatial distribution. *Brain Res.* 1984;322(1):1–7.
20. Kolb H, Cuenca N, Wang HH, Dekorver L. The synaptic organization of the dopaminergic amacrine cell in the cat retina. *J. Neurocytol.* 1990;19(3):343–366.
21. Jackson CR, Ruan G-X, Aseem F, et al. Retinal dopamine mediates multiple dimensions of light-adapted vision. *J. Neurosci.* 2012;32(27):9359–9368.
22. Beach TG, Adler CH, Sue LI, et al. Arizona Study of Aging and Neurodegenerative Disorders and Brain and Body Donation Program. *Neuropathology* 2015;35(4):354–389.
23. Beach TG, Sue LI, Walker DG, et al. The Sun Health Research Institute Brain Donation Program: Description and Experience, 1987–2007. *Cell Tissue Bank.* 2008;9(3):229–245.
24. Gelb D, Oliver E, Gilman S. Diagnostic criteria for parkinson disease. *Arch. Neurol.* 1999;56(1):33–39.

25. Provencio I, Rodriguez IR, Jiang G, et al. A novel human opsin in the inner retina. *J Neurosci* 2000;20(2):600–605.
26. Fasoli A, Dang J, Johnson JS, et al. Somatic and neuritic spines on tyrosine hydroxylase–immunopositive cells of rat retina. *J. Comp. Neurol.* 2017;525(7):1707–1730.
27. Keeley PW, Reese BE. Morphology of dopaminergic amacrine cells in the mouse retina: independence from homotypic interactions. *J. Comp. Neurol.* 2010;518(8):1220–1231.
28. Cuenca N, Deng P, Linberg KA, et al. The neurons of the ground squirrel retina as revealed by immunostains for calcium binding proteins and neurotransmitters. *J. Neurocytol.* 2002;31(8–9):649–666.
29. Dacey DM. The dopaminergic amacrine cell. *J. Comp. Neurol.* 1990;301(3):461–489.
30. Guimarães PZ, Hokoç JN. Tyrosine hydroxylase expression in the Cebus monkey retina. *Vis. Neurosci.* 1997;14(4):705–715.
31. Lee SCS, Weltzien F, Madigan MC, et al. Identification of A II amacrine, displaced amacrine, and bistratified ganglion cell types in human retina with antibodies against calretinin. *J. Comp. Neurol.* 2016;524(1):39–53.
32. Cuenca N, Ortuño-Lizarán I, Pinilla I. Cellular Characterization of OCT and Outer Retinal Bands Using Specific Immunohistochemistry Markers and Clinical Implications. *Ophthalmology* 2018;125(3):407–422.
33. O’Brien JJ, Chen X, Macleish PR, et al. Photoreceptor coupling mediated by connexin36 in the primate retina. *J. Neurosci.* 2012;32(13):4675–4687.
34. Rollag MD, Berson DM, Provencio I. Melanopsin, ganglion-cell photoreceptors, and mammalian photoentrainment. *J. Biol. Rhythms* 2003;18(3):227–234.
35. Wickham H. *ggplot2: Elegant Graphics for Data Analysis*. Springer-Verlag New York;

2016.

36. Wang HH, Cuenca N, Kolb H. Development of morphological types and distribution patterns of amacrine cells immunoreactive to tyrosine hydroxylase in the cat retina. *Vis. Neurosci.* 1990;4(2):159–175.
37. Dowling JE. Dopamine: a retinal neuromodulator? *Trends Neurosci.* 1986;9:236–240.
38. Witkovsky P, Deary A. Functional roles of dopamine in the vertebrate retina. *Prog. Retin. Res.* 1991;11:247–292.
39. Kolb H, Cuenca N, Dekorver L. Postembedding immunocytochemistry for GABA and glycine reveals the synaptic relationships of the dopaminergic amacrine cell of the cat retina. *J. Comp. Neurol.* 1991;310(2):267–284.
40. Witkovsky P. Dopamine and retinal function. *Doc. Ophthalmol.* 2004;108(1):17–40.
41. Popova E. Role of dopamine in distal retina. *J. Comp. Physiol. A. Neuroethol. Sens. Neural. Behav. Physiol.* 2014;200(5):333–58.
42. Bloomfield SA. Plasticity of AII amacrine cell circuitry in the mammalian retina. *Prog. Brain Res.* 2001;131:185–200.
43. Bloomfield SA, Dacheux RF. Rod vision: pathways and processing in the mammalian retina. *Prog. Retin. Eye Res.* 2001;20(3):351–384.
44. Kolb H, Zhang L, Dekorver L, Cuenca N. A new look at calretinin-immunoreactive amacrine cell types in the monkey retina. *J. Comp. Neurol.* 2002;453(2):168–184.
45. Strettoi E, Raviola E, Dacheux RF. Synaptic connections of the narrow-field, bistratified rod amacrine cell (AII) in the rabbit retina. *J. Comp. Neurol.* 1992;325(2):152–168.
46. Trexler EB, Li W, Mills SL, Massey SC. Coupling from AII amacrine cells to ON cone bipolar cells is bidirectional. *J. Comp. Neurol.* 2001;437(4):408–422.
47. Giannoccaro MP, La Morgia C, Rizzo G, Carelli V. Mitochondrial DNA and primary

mitochondrial dysfunction in Parkinson's disease. *Mov. Disord.* 2017;32(3):346–363.

48. Nguyen-Legros J. Functional neuroarchitecture of the retina: hypothesis on the dysfunction of retinal dopaminergic circuitry in Parkinson's disease. *Surg. Radiol. Anat.* 1988;10(2):137–144.
49. Adam CR, Shrier E, Ding Y, et al. Correlation of Inner Retinal Thickness Evaluated by Spectral-Domain Optical Coherence Tomography and Contrast Sensitivity in Parkinson disease. *J. Neuro-Ophthalmology* 2013;33(2):137–142.
50. Harnois C, Di Paolo T. Decreased dopamine in the retinas of patients with Parkinson's disease. *Invest. Ophthalmol. Vis. Sci.* 1990;31(11):2473–2475.
51. Wong C, Ishibashi T, Tucker G, Hamasaki D. Responses of the pigmented rabbit retina to NMPTP, a chemical inducer of parkinsonism. *Exp. Eye Res.* 1985;40(4):509–519.
52. Ghilardi MF, Chung E, Bodis-Wollner I, et al. Systemic 1-methyl,4-phenyl,1-2-3-6-tetrahydropyridine (MPTP) administration decreases retinal dopamine content in primates. *Life Sci.* 1988;43(3):255–262.
53. Mariani AP, Neff NH, Hadjiconstantinou M. 1-Methyl-4-phenyl-1,2,3,6-tetrahydropyridine (MPTP) treatment decreases dopamine and increases lipofuscin in mouse retina. *Neurosci. Lett.* 1986;72(2):221–226.
54. Tatton WG, Kwan MM, Verrier MC, et al. MPTP produces reversible disappearance of tyrosine hydroxylase-containing retinal amacrine cells. *Brain Res.* 1990;527(1):21–31.
55. Peoples C, Shaw VE, Stone J, et al. Survival of Dopaminergic Amacrine Cells after Near-Infrared Light Treatment in MPTP-Treated Mice. *ISRN Neurol.* 2012;2012:850150.
56. Cuenca N, Herrero M-T, Angulo A, et al. Morphological impairments in retinal neurons of the scotopic visual pathway in a monkey model of Parkinson's disease. *J. Comp.*

Neurol. 2005;493(2):261–273.

57. Esteve-Rudd J, Fernández-Sánchez L, Lax P, et al. Rotenone induces degeneration of photoreceptors and impairs the dopaminergic system in the rat retina. *Neurobiol. Dis.* 2011;44(1):102–115.
58. Biehlmaier O, Alam M, Schmidt WJ. A rat model of Parkinsonism shows depletion of dopamine in the retina. *Neurochem. Int.* 2007;50(1):189–195.
59. Meng T, Zheng ZH, Liu TT, Lin L. Contralateral retinal dopamine decrease and melatonin increase in progression of hemiparkinsonium rat. *Neurochem. Res.* 2012;37(5):1050–1056.
60. Marrocco E, Esposito F, Tarallo V, et al.  $\alpha$ -synuclein in the retina leads to degeneration of dopamine amacrine cells impairing vision. *bioRxiv* 2019;
61. Beach TG, Carew J, Serrano G, et al. Phosphorylated  $\alpha$ -synuclein-immunoreactive retinal neuronal elements in Parkinson's disease subjects. *Neurosci. Lett.* 2014;571:34–38.
62. Armstrong RA. Visual Dysfunction in Parkinson's Disease. *Int. Rev. Neurobiol.* 2017;134:921–946.
63. Guo L, Normando EM, Shah PA, et al. Oculo-visual abnormalities in Parkinson's disease: Possible value as biomarkers. *Mov. Disord.* 2018;33(9):1390–1406.
64. Safranow K. Ophthalmological Features of Parkinson Disease. *Med. Sci. Monit.* 2014;20:2243–2249.
65. Nguyen-Legros J, Versaux-Botteri C, Vernier P. Dopamine receptor localization in the mammalian retina. *Mol. Neurobiol.* 1999;19(3):181–204.
66. Holopigian K, Clewner L, Seiple W, Kupersmith MJ. The effects of dopamine blockade on the human flash electroretinogram. *Doc. Ophthalmol.* 1994;86(1):1–10.

67. Inzelberg R, Ramirez JA, Nisipeanu P, Ophir A. Retinal nerve fiber layer thinning in Parkinson disease. *Vision Res.* 2004;44(24):2793–2797.
68. Willis GL, Moore C, Armstrong SM. Parkinson's Disease, Lights and Melanocytes: Looking Beyond the Retina. *Sci. Rep.* 2015;4(1):3921.
69. Willis GL. Intraocular microinjections repair experimental Parkinson's disease. *Brain Res.* 2008;1217:119–131.
70. Videnovic A, Klerman EB, Wang W, et al. Timed Light Therapy for Sleep and Daytime Sleepiness Associated With Parkinson Disease. *JAMA Neurol.* 2017;74(4):411.
71. Li Z, Tian T. Light Therapy Promoting Dopamine Release by Stimulating Retina in Parkinson Disease. *JAMA Neurol.* 2017;74(10):1267.
72. Videnovic A, Klerman EB, Zee PC. Light therapy promoting dopamine release by stimulating retina in parkinson disease - Reply. *JAMA Neurol.* 2017;74(10):1268–1269.



## Figure legends

**Fig. 1** Dopaminergic cells display an impaired morphology in PD. Dopaminergic cells (green) in healthy retinas (A) have long thin dendrites that create a dense plexus with ring structures (arrows) surrounding their post-synaptic cell bodies. In PD (B), dendrites are shorter and display some swollen regions (arrowheads), a sign of degeneration. Their plexus is less continuous, and it has lost the typical dopaminergic rings. In transversal sections, the density of the dopaminergic plexus can be observed in control (C) and PD (D) retinas. Dopaminergic plexus in control subjects (C) is much thicker, denser and more continuous than in PD patients (D). In addition, while a dopaminergic plexus at IPL S3 can be identified in controls, it is almost lost in PD, as are the few dopaminergic projections to S5 (arrowheads). Dopaminergic projections towards the outer retina (OPL and ONL) can be observed in controls (C) but are strongly reduced in PD (D) (arrows). n=5 control, n=8 PD. Scale bar A-D:10  $\mu\text{m}$ .

**Fig. 2** Density of dopaminergic amacrine cells is reduced in PD. Color-coded density maps of dopaminergic cells in the macular region (temporal-central pieces) of control (A) and PD (B) reflect the decreased dopaminergic density in patients. Each dopaminergic cell is represented by a white or black dot and, in the color gradient, yellow represents the highest cell density (45 cells/mm<sup>2</sup>) and dark blue the lowest (0 cells/mm<sup>2</sup>). Insets in (A) and (B) show high magnification images of the parafovea where changes in cell number between groups can be observed. Confocal images of dopaminergic amacrine cells in the parafovea of control (C) and PD (D) also show the decline in cell number observed in the disease. Dopaminergic cell density is highest at the parafovea, concentrically decreases towards higher eccentricities, and it is reduced in PD compared to controls in all the locations tested (E). In the temporal-central quadrant the dopaminergic density decreased from 20.2 cells/mm<sup>2</sup> in controls to 13.1 cells/mm<sup>2</sup> in PD,

changing from 45.1 in controls to 19.2 cells/mm<sup>2</sup> in PD in the parafovea, from 29.7 cells/mm<sup>2</sup> to 14.4 cells/mm<sup>2</sup> in the perifovea, and from 18.5 cells/mm<sup>2</sup> to 12.9 cells/mm<sup>2</sup> in the next 3mm.. In the superonasal quadrant, density maps of a representative area show the differences in dopaminergic cell density between control (F) and PD (G) and how the density is gradually reduced towards the periphery. This density is significantly reduced in PD, changing from 18.4 cells/mm<sup>2</sup> in the retina of healthy individuals to 10.8 cells/mm<sup>2</sup> in the retina of PD patients, and differences are maintained along the retina: from 2 to 7 mm to optic nerve dopaminergic cells change from 19.4 cells/mm<sup>2</sup> in controls to 13.4 cells/mm<sup>2</sup> in PD, from 7 to 11 mm to optic nerve it is reduced from 17.3 cells/mm<sup>2</sup> in controls to 12.8 cells/mm<sup>2</sup> in PD, and in the most peripheral region, from 11 to 16 mm to the optic nerve, dopaminergic density diminishes from 14.4 cells/mm<sup>2</sup> in controls to 8.8 cells/mm<sup>2</sup> in PD, being statistically significant in all cases. ON: Optic Nerve; Fv: Fovea. A-E: n=3 control, n=2 PD; F-H: n=5 control, n=8 PD. Scale bar A-B, F-G: 1mm; C-D: 20  $\mu$ m. \*: P<0.05; \*\*: P<0.01.

**Fig. 3** All amacrine cells maintain their cell density in PD although their dopaminergic inputs are reduced. Double immunostaining using tyrosine hydroxylase (TH, green) and calretinin (CR, red) shows the interactions between dopaminergic (green) and AII (red) amacrine cells. In control retinas (A), dopaminergic cells make several synaptic contacts around AII soma (arrows), which are severely lost in PD (B). High magnification images show the contacts and the ring structures in controls (C, D) and PD (E, F) (arrowheads). Their quantification revealed a significant loss of dopaminergic contacts per AII cell, from  $9.3\pm 0.2$  in controls to  $3.7\pm 0.8$  in PD (G) but no differences in the number of AII amacrine cells was observed (H). n=4 control, n=7 PD, H: 20 different frames per retina. Scale bar A-B: 20  $\mu$ m; C-F: 5  $\mu$ m; \*\*: P<0.01; n.s.: non-significant

**Fig. 4** AII amacrine cells loss mitochondria in their lobular appendages in PD. Calretinin (CR) shows AII amacrine cells (red) and cytochrome C (CytC) shows mitochondria in control (A) and PD (B) retinas. AII amacrine cells (red) present small dendrites that stratify close to the cell body in both sublamina a and b of the IPL (A). In PD, their typical morphology has been partially disrupted, showing an apparent loss of lobular appendages and stratification. Also, healthy subjects have big and abundant mitochondria within the AII lobular appendages (C, arrows) while fewer and smaller mitochondria are found in the retina of PD (D, arrows). Higher magnification images of the areas indicated by dotted lines show differences in mitochondria size and number between controls, where lobular appendages are full of big mitochondria (E, arrows) and PD, where mitochondria are small, sparse (F, arrows) and some lobular appendages seem empty. n=3 control, n=5 PD. Scale bar A-D: 10  $\mu\text{m}$ ; E-F: 5  $\mu\text{m}$

**Fig. 5** AII amacrine cells in PD loss connexin 36 at the ON *sublamina* of the IPL. In healthy controls (A), AII (calretinin, CR, red) gap junctions are mediated by connexin 36 (Cx36, green), which is abundant at the IPL ON *sublamina*. In PD (B), connexin 36 is reduced, probably altering gap junctions. (C) and (D) are the same images as (A) and (B) respectively but showing the green channel alone, to properly observe the connexin 36 reduction in PD (D). (E-F) are high magnification images of (A-B) dotted areas. Notice the altered morphology of AII cells (less lobular appendages and impaired stratification) and the reduction in connexin 36 in PD (F) compared to controls (E). (G-H) images display the green channel from (E-F) images and are high magnification of (C-D); they show the strong decline in connexin 36 in the sublamina ON of the IPL in PD (H) compared to controls (G). n=3 control, n=5 PD Scale bar: A-D: 10  $\mu\text{m}$ ; E-F: 5  $\mu\text{m}$

**Fig. 6** Dopaminergic synaptic contacts to melanopsin retinal ganglion cells are reduced in PD. In controls, melanopsin cells (red) display their normal morphology (A), while in PD cell dendrites are less complex, having lower number of branches and shorter dendrites (B). Also, controls display a dense dopaminergic plexus (green) (C), that is reduced in PD (D). In high-magnification images, details of synaptic contacts of dopaminergic cells in melanopsin dendrites can be observed (E-H), showing that controls (E, F) have a higher number of contacts than PD (G, H). Its quantification revealed a loss of dopaminergic synaptic contacts in melanopsin dendrites: from  $70 \pm 14$  contacts per  $100 \mu\text{m}$  in controls to  $43 \pm 9$  contacts per  $100 \mu\text{m}$  in PD ( $P < 0.0001$ ) (i).  $n=3$  control,  $n=3$  PD, 15 different frames per retina. Scale bar: A-D:  $20 \mu\text{m}$ ; E-H:  $1 \mu\text{m}$

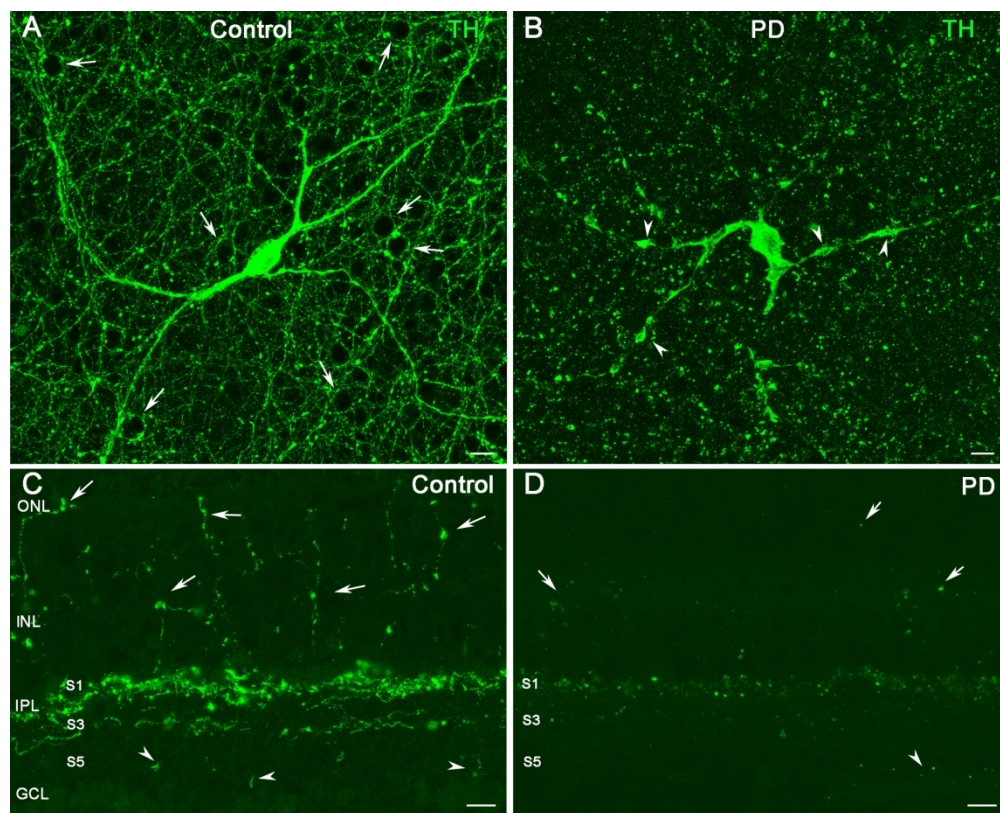


Fig. 1 Dopaminergic cells display an impaired morphology in PD. Dopaminergic cells (green) in healthy retinas (A) have long thin dendrites that create a dense plexus with ring structures (arrows) surrounding their post-synaptic cell bodies. In PD (B), dendrites are shorter and display some swollen regions (arrowheads), a sign of degeneration. Their plexus is less continuous, and it has lost the typical dopaminergic rings. In transversal sections, the density of the dopaminergic plexus can be observed in control (C) and PD (D) retinas. Dopaminergic plexus in control subjects (C) is much thicker, denser and more continuous than in PD patients (D). In addition, while a dopaminergic plexus at IPL S3 can be identified in controls, it is almost lost in PD, as are the few dopaminergic projections to S5 (arrowheads). Dopaminergic projections towards the outer retina (OPL and ONL) can be observed in controls (C) but are strongly reduced in PD (D) (arrows). n=5 control, n=8 PD. Scale bar A-D:10  $\mu$ m.

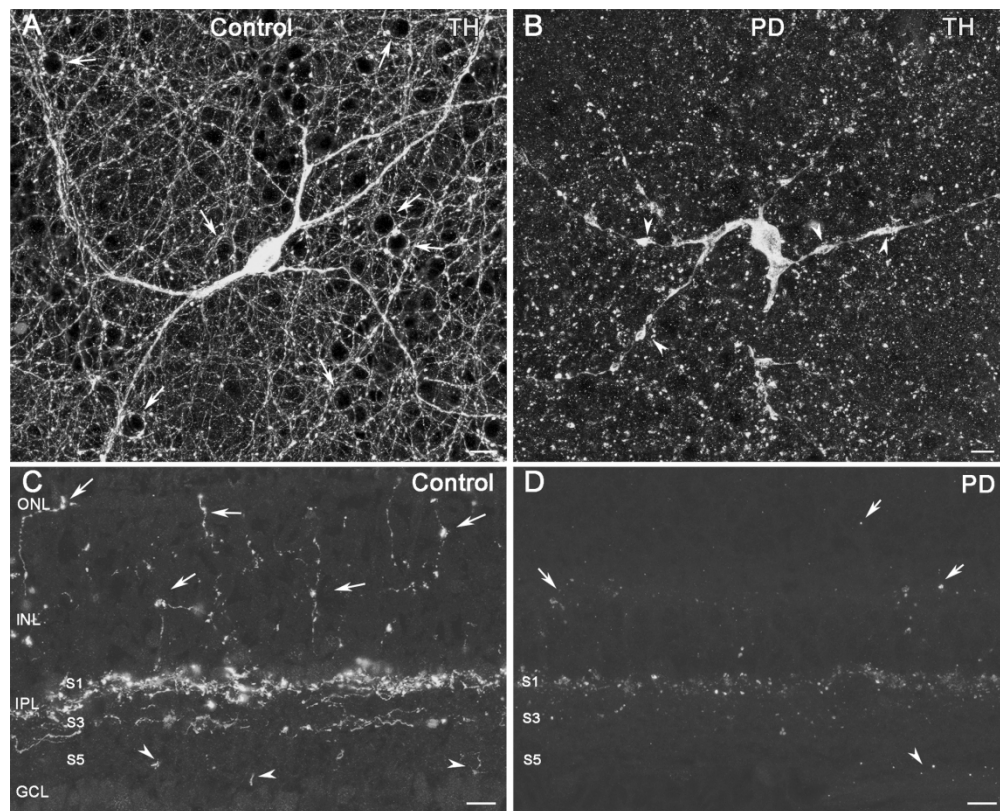


Fig. 1 Dopaminergic cells display an impaired morphology in PD. Dopaminergic cells (green) in healthy retinas (A) have long thin dendrites that create a dense plexus with ring structures (arrows) surrounding their post-synaptic cell bodies. In PD (B), dendrites are shorter and display some swollen regions (arrowheads), a sign of degeneration. Their plexus is less continuous, and it has lost the typical dopaminergic rings. In transversal sections, the density of the dopaminergic plexus can be observed in control (C) and PD (D) retinas. Dopaminergic plexus in control subjects (C) is much thicker, denser and more continuous than in PD patients (D). In addition, while a dopaminergic plexus at IPL S3 can be identified in controls, it is almost lost in PD, as are the few dopaminergic projections to S5 (arrowheads). Dopaminergic projections towards the outer retina (OPL and ONL) can be observed in controls (C) but are strongly reduced in PD (D) (arrows). n=5 control, n=8 PD. Scale bar A-D:10  $\mu$ m.

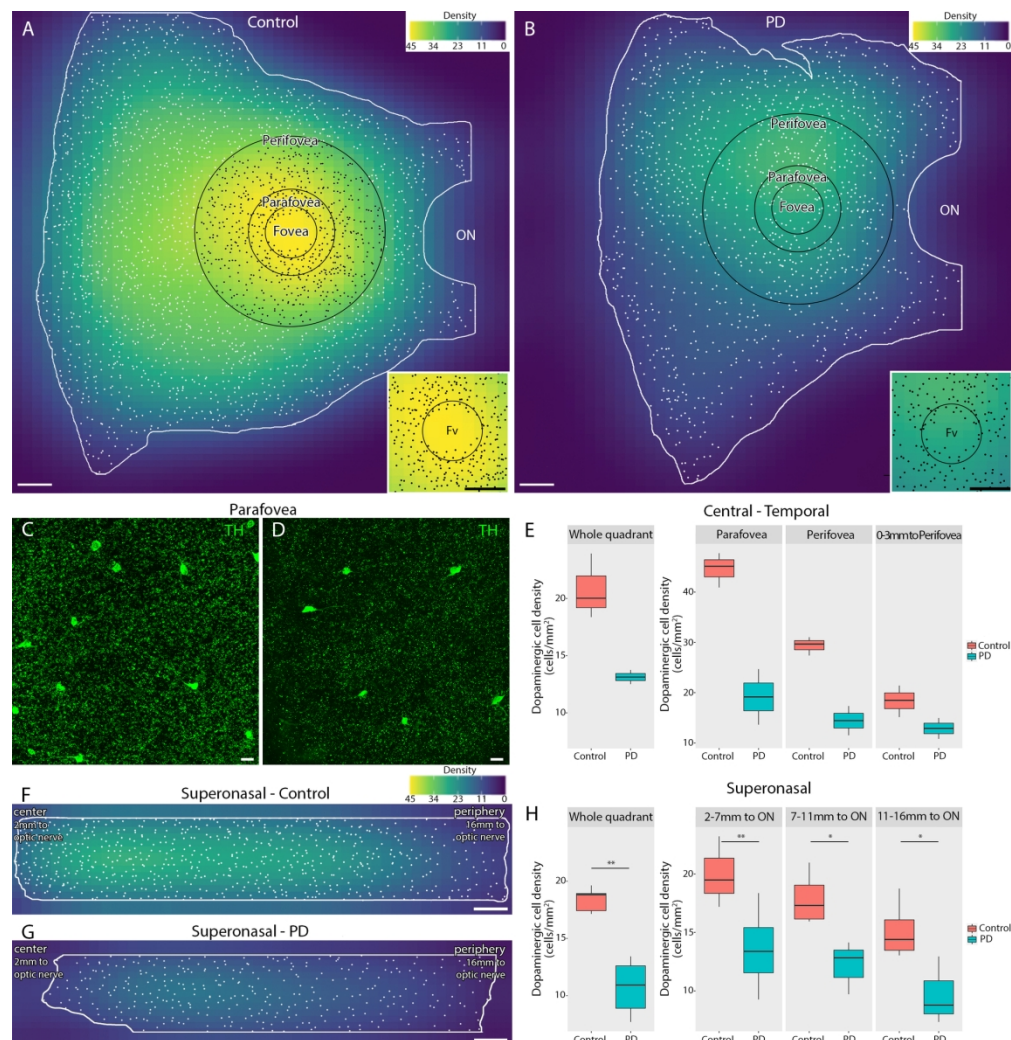


Fig. 2 Density of dopaminergic amacrine cells is reduced in PD. Color-coded density maps of dopaminergic cells in the macular region (temporal-central pieces) of control (A) and PD (B) reflect the decreased dopaminergic density in patients. Each dopaminergic cell is represented by a white or black dot and, in the color gradient, yellow represents the highest cell density (45 cells/mm<sup>2</sup>) and dark blue the lowest (0 cells/mm<sup>2</sup>). Insets in (A) and (B) show high magnification images of the parafovea where changes in cell number between groups can be observed. Confocal images of dopaminergic amacrine cells in the parafovea of control (C) and PD (D) also show the decline in cell number observed in the disease. Dopaminergic cell density is highest at the parafovea, concentrically decreases towards higher eccentricities, and it is reduced in PD compared to controls in all the locations tested (E). In the temporal-central quadrant the dopaminergic density decreased from 20.2 cells/mm<sup>2</sup> in controls to 13.1 cells/mm<sup>2</sup> in PD, changing from 45.1 in controls to 19.2 cells/mm<sup>2</sup> in PD in the parafovea, from 29.7 cells/mm<sup>2</sup> to 14.4 cells/mm<sup>2</sup> in the perifovea, and from 18.5 cells/mm<sup>2</sup> to 12.9 cells/mm<sup>2</sup> in the next 3mm. In the superonasal quadrant, density maps of a representative area show the differences in dopaminergic cell density between control (F) and PD (G) and how the density is gradually reduced towards the periphery. This density is significantly reduced in PD, changing from 18.4 cells/mm<sup>2</sup> in the retina of healthy individuals to 10.8 cells/mm<sup>2</sup> in the retina of PD patients, and differences are maintained along the retina: from 2 to 7 mm to optic nerve dopaminergic cells change from 19.4 cells/mm<sup>2</sup> in controls to 13.4 cells/mm<sup>2</sup> in PD, from 7 to 11 mm to optic nerve it is reduced from 17.3 cells/mm<sup>2</sup> in controls to 12.8 cells/mm<sup>2</sup> in PD, and in the most peripheral region, from 11 to 16 mm to the optic nerve, dopaminergic density diminishes from 14.4 cells/mm<sup>2</sup> in controls to 8.8

cells/mm<sup>2</sup> in PD, being statistically significant in all cases. ON: Optic Nerve; Fv: Fovea. A-E: n=3 control, n=2 PD; F-H: n=5 control, n=8 PD. Scale bar A-B, F-G: 1mm; C-D: 20  $\mu$ m. \*: P<0.05; \*\*: P<0.01.



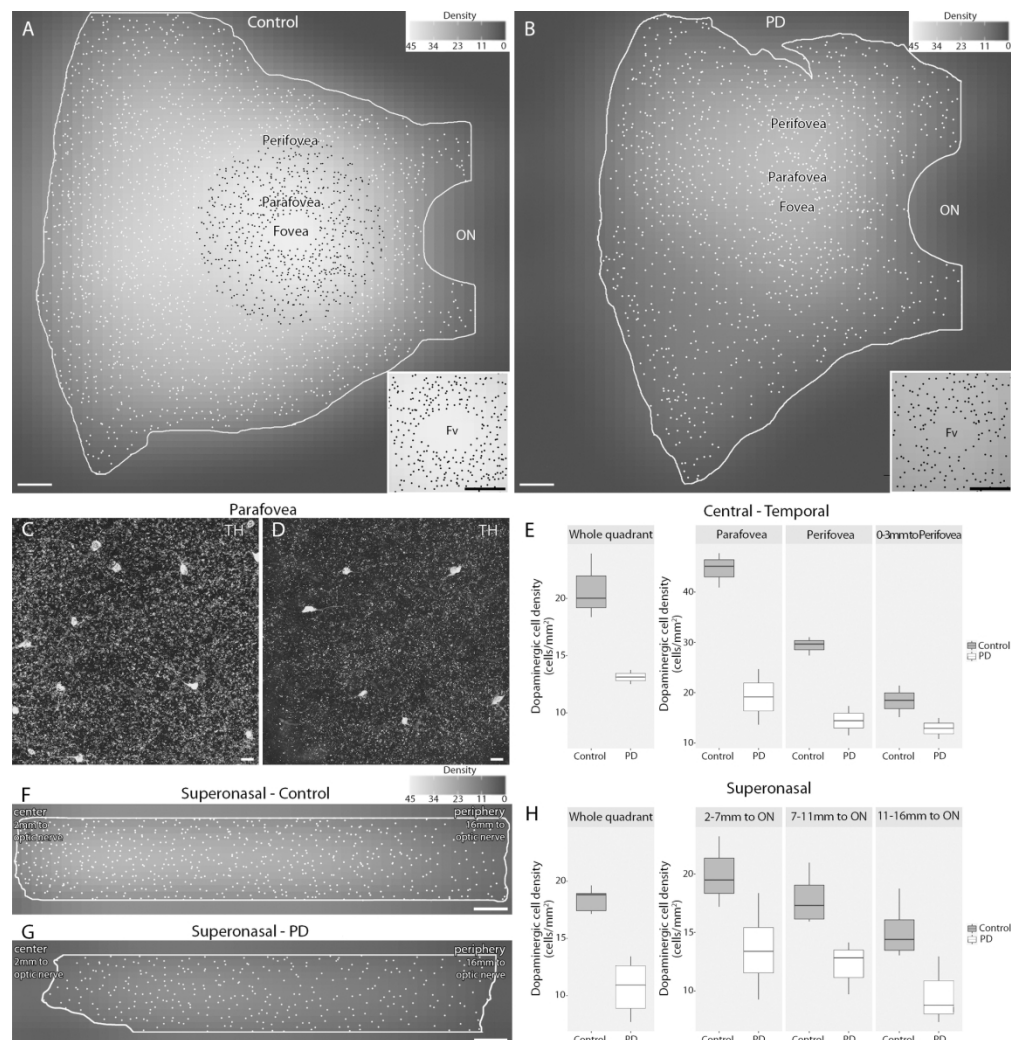


Fig. 2 Density of dopaminergic amacrine cells is reduced in PD. Color-coded density maps of dopaminergic cells in the macular region (temporal-central pieces) of control (A) and PD (B) reflect the decreased dopaminergic density in patients. Each dopaminergic cell is represented by a white or black dot and, in the color gradient, yellow represents the highest cell density (45 cells/mm<sup>2</sup>) and dark blue the lowest (0 cells/mm<sup>2</sup>). Insets in (A) and (B) show high magnification images of the parafovea where changes in cell number between groups can be observed. Confocal images of dopaminergic amacrine cells in the parafovea of control (C) and PD (D) also show the decline in cell number observed in the disease. Dopaminergic cell density is highest at the parafovea, concentrically decreases towards higher eccentricities, and it is reduced in PD compared to controls in all the locations tested (E). In the temporal-central quadrant the dopaminergic density decreased from 20.2 cells/mm<sup>2</sup> in controls to 13.1 cells/mm<sup>2</sup> in PD, changing from 45.1 in controls to 19.2 cells/mm<sup>2</sup> in PD in the parafovea, from 29.7 cells/mm<sup>2</sup> to 14.4 cells/mm<sup>2</sup> in the perifovea, and from 18.5 cells/mm<sup>2</sup> to 12.9 cells/mm<sup>2</sup> in the next 3mm. In the superonasal quadrant, density maps of a representative area show the differences in dopaminergic cell density between control (F) and PD (G) and how the density is gradually reduced towards the periphery. This density is significantly reduced in PD, changing from 18.4 cells/mm<sup>2</sup> in the retina of healthy individuals to 10.8 cells/mm<sup>2</sup> in the retina of PD patients, and differences are maintained along the retina: from 2 to 7 mm to optic nerve dopaminergic cells change from 19.4 cells/mm<sup>2</sup> in controls to 13.4 cells/mm<sup>2</sup> in PD, from 7 to 11 mm to optic nerve it is reduced from 17.3 cells/mm<sup>2</sup> in controls to 12.8 cells/mm<sup>2</sup> in PD, and in the most peripheral region, from 11 to 16 mm to the optic nerve, dopaminergic density diminishes from 14.4 cells/mm<sup>2</sup> in controls to 8.8

cells/mm<sup>2</sup> in PD, being statistically significant in all cases. ON: Optic Nerve; Fv: Fovea. A-E: n=3 control, n=2 PD; F-H: n=5 control, n=8 PD. Scale bar A-B, F-G: 1mm; C-D: 20  $\mu$ m. \*: P<0.05; \*\*: P<0.01.

view

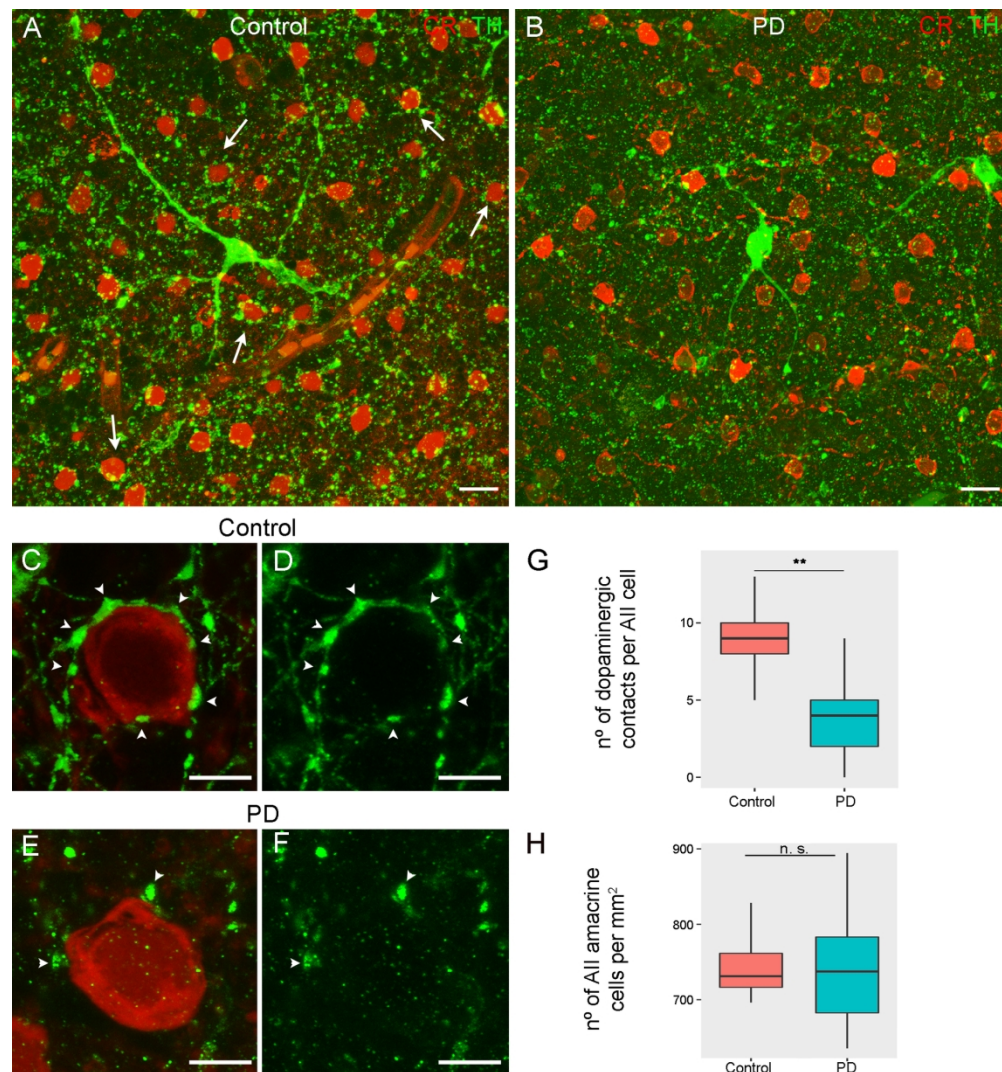


Fig. 3 AII amacrine cells maintain their cell density in PD although their dopaminergic inputs are reduced. Double immunostaining using tyrosine hydroxylase (TH, green) and calretinin (CR, red) shows the interactions between dopaminergic (green) and AII (red) amacrine cells. In control retinas (A), dopaminergic cells make several synaptic contacts around AII soma (arrows), which are severely lost in PD (B). High magnification images show the contacts and the ring structures in controls (C, D) and PD (E, F) (arrowheads). Their quantification revealed a significant loss of dopaminergic contacts per AII cell, from  $9.3 \pm 0.2$  in controls to  $3.7 \pm 0.8$  in PD (G) but no differences in the number of AII amacrine cells was observed (H).  $n=4$  control,  $n=7$  PD, H: 20 different frames per retina. Scale bar A-B:  $20 \mu\text{m}$ ; C-F:  $5 \mu\text{m}$ ; \*\*:  $P < 0.01$ ; n.s.: non-significant

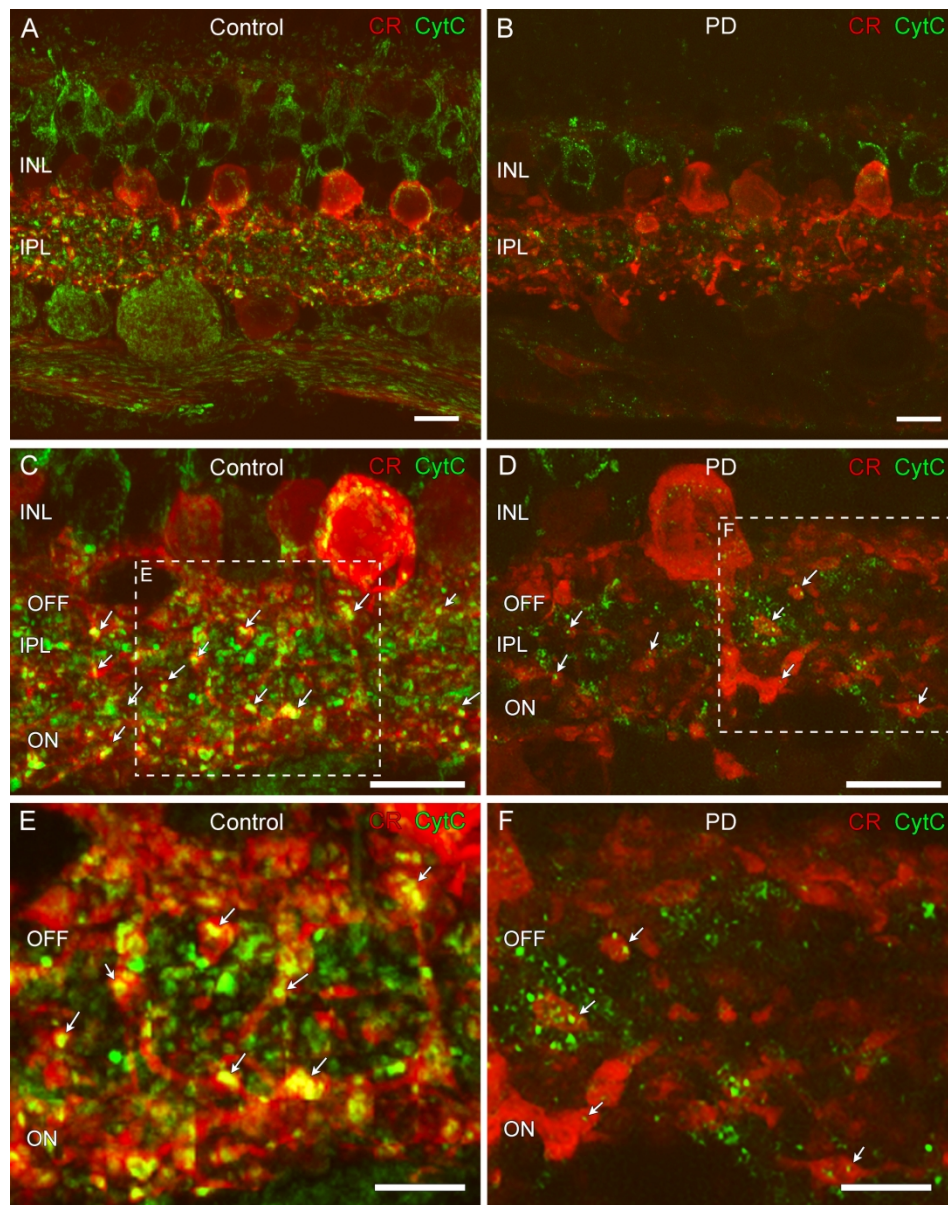


Fig. 4 AII amacrine cells lose mitochondria in their lobular appendages in PD. Calretinin (CR) shows AII amacrine cells (red) and cytochrome C (CytC) shows mitochondria in control (A) and PD (B) retinas. AII amacrine cells (red) present small dendrites that stratify close to the cell body in both sublamina a and b of the IPL (A). In PD, their typical morphology has been partially disrupted, showing an apparent loss of lobular appendages and stratification. Also, healthy subjects have big and abundant mitochondria within the AII lobular appendages (C, arrows) while fewer and smaller mitochondria are found in the retina of PD (D, arrows). Higher magnification images of the areas indicated by dotted lines show differences in mitochondria size and number between controls, where lobular appendages are full of big mitochondria (E, arrows) and PD, where mitochondria are small, sparse (F, arrows) and some lobular appendages seem empty. n=3 control, n=5 PD. Scale bar A-D: 10  $\mu$ m; E-F: 5  $\mu$ m

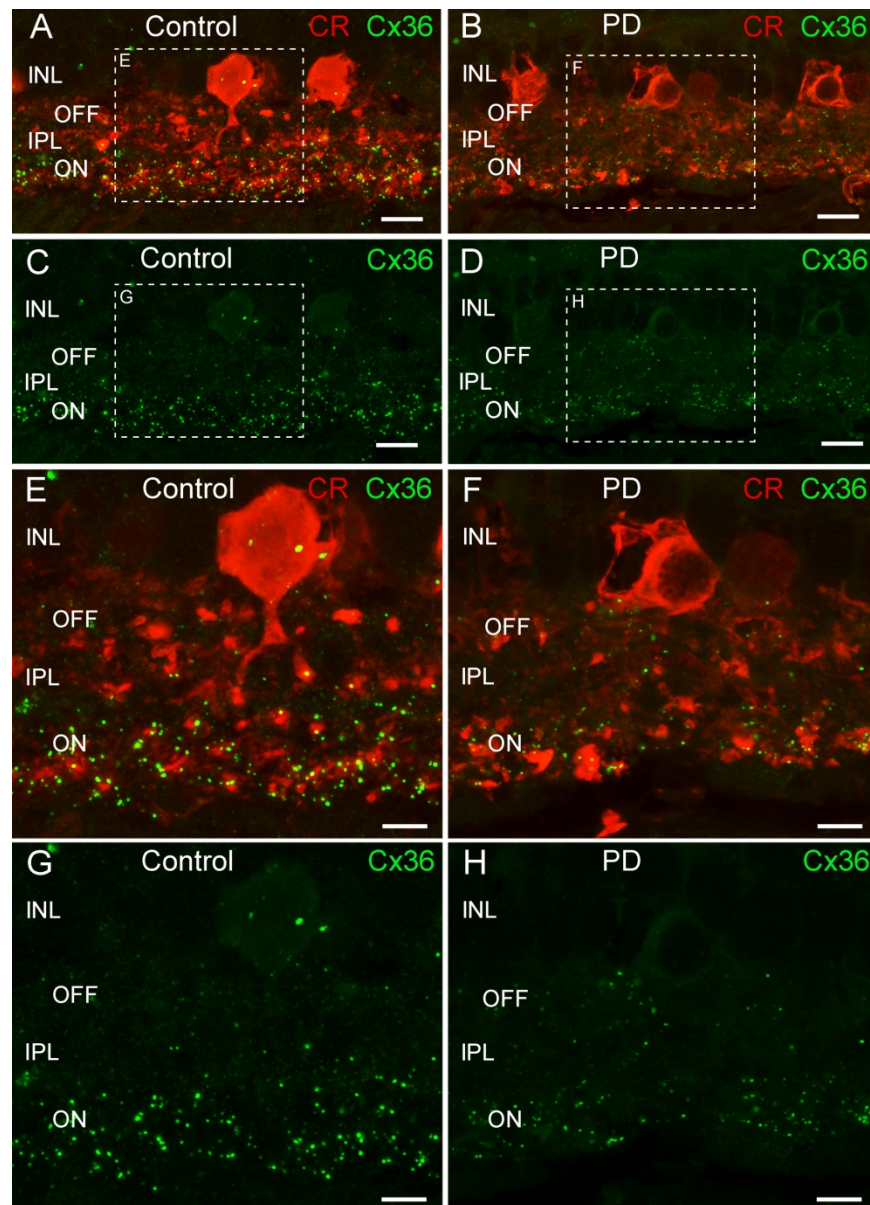


Fig. 5 AII amacrine cells in PD loss connexin 36 at the ON sublamina of the IPL. In healthy controls (A), AII (calretinin, CR, red) gap junctions are mediated by connexin 36 (Cx36, green), which is abundant at the IPL ON sublamina. In PD (B), connexin 36 is reduced, probably altering gap junctions. (C) and (D) are the same images as (A) and (B) respectively but showing the green channel alone, to properly observe the connexin 36 reduction in PD (D). (E-F) are high magnification images of (A-B) dotted areas. Notice the altered morphology of AII cells (less lobular appendages and impaired stratification) and the reduction in connexin 36 in PD (F) compared to controls (E). (G-H) images display the green channel from (E-F) images and are high magnification of (C-D); they show the strong decline in connexin 36 in the sublamina ON of the IPL in PD (H) compared to controls (G). n=3 control, n=5 PD Scale bar: A-D: 10  $\mu$ m; E-F: 5  $\mu$ m

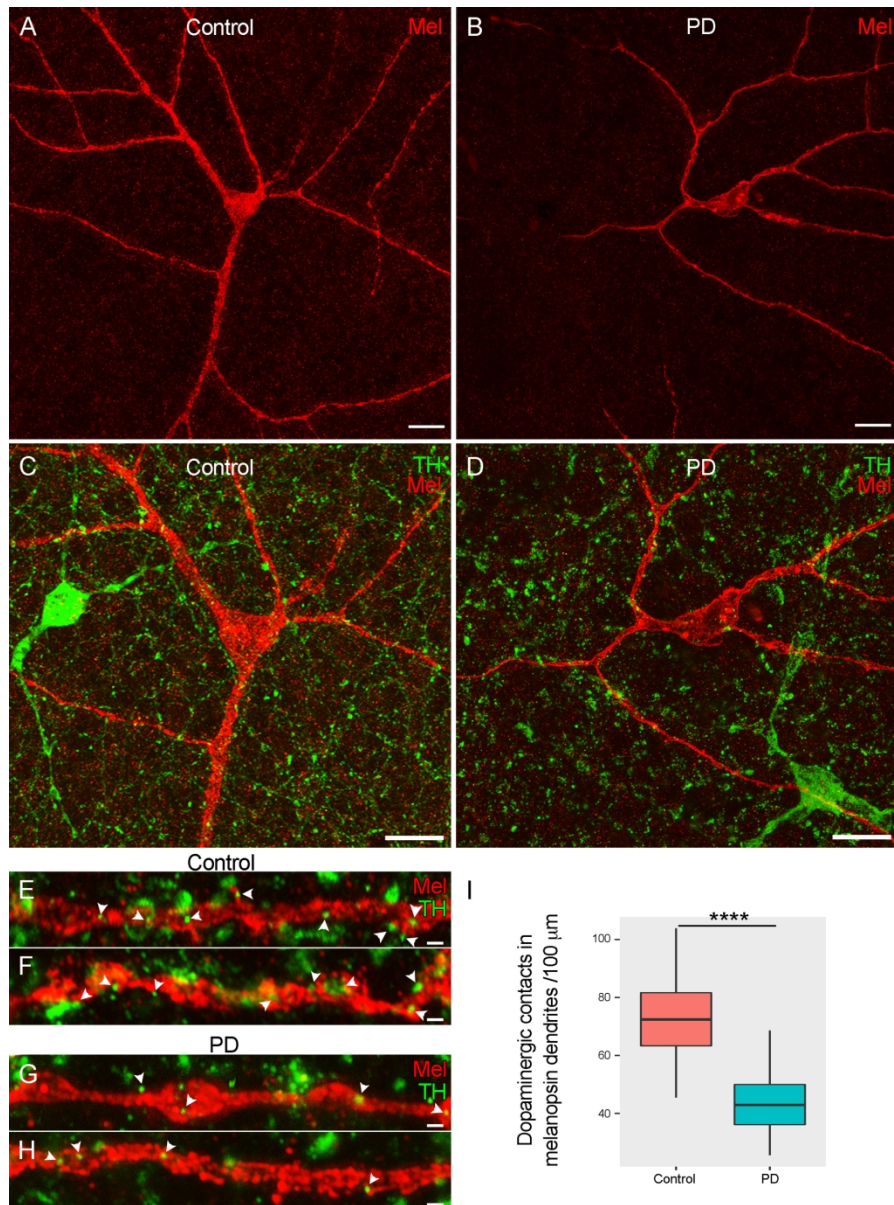


Fig. 6 Dopaminergic synaptic contacts to melanopsin retinal ganglion cells are reduced in PD. In controls, melanopsin cells (red) display their normal morphology (A), while in PD cell dendrites are less complex, having lower number of branches and shorter dendrites (B). Also, controls display a dense dopaminergic plexus (green) (C), that is reduced in PD (D). In high-magnification images, details of synaptic contacts of dopaminergic cells in melanopsin dendrites can be observed (E-H), showing that controls (E, F) have a higher number of contacts than PD (G, H). Its quantification revealed a loss of dopaminergic synaptic contacts in melanopsin dendrites: from  $70 \pm 14$  contacts per  $100 \mu\text{m}$  in controls to  $43 \pm 9$  contacts per  $100 \mu\text{m}$  in PD ( $P < 0.0001$ ) (i).  $n=3$  control,  $n=3$  PD, 15 different frames per retina. Scale bar: A-D:  $20 \mu\text{m}$ ; E-H:  $1 \mu\text{m}$